JOURNAL OF APPLIED ELECTROCHEMISTRY 10 (1980) 481–488

Retardation of electrolytic mass transport in collinear electric-magnetic fields

T. Z. FAHIDY, T. S. RUTHERFORD*

Department of Chemical Engineering, University of Waterloo, Waterloo, Ontario, Canada

Received 6 August 1979

The adverse effect of parallel magnetic and electric fields perpendicular to horizontal electrodes facing upwards in combined natural and forced convection was studied experimentally. The results are interpreted in terms of convective-diffusion models modified for the magnetic field interaction.

Nomenclature

B	magnetic flux density vector
B_0	magnitude of its vertically imposed value
c	concentration of the electrolyte
D	electrolyte diffusion coefficient
d	anode-cathode separation distance
d_e	equivalent channel diameter
F	Faraday's constant
i	cathode current density
i	current density vector
L	electrode length
M	molar mass of electrolyte
n	interaction parameter
p	pressure drop
(Ra)	Rayleigh number
(Re)	Reynolds number (characteristic length: d_e)
(Sc)	Schmidt number
(Sh)	Sherwood number
v	velocity
x	co-ordinate along reactor length
y	co-ordinate perpendicular to electrode surfaces
z	valency
α	densification coefficient
γ	shape factor
$\bar{\gamma}$	magnetic interaction parameter
θ	dimensionless electrolyte concentration
λ	characteristic length
ν	kinematic viscosity
ρ	density
σ	electric conductance
τ	residence time

Subscripts

FC	related to forced convection
NC	related to natural convection
L	related to electrode length
x, y	related to the x and y co-ordinates
∞	related to fully developed (bulk) conditions

Superscript

0	related to the absence of the magnetic field

1. Introduction

The enhancing effect of magnetic fields, imposed upon d.c. electric fields, on electrolytic mass transport rates has been amply documented in the recent literature. Under otherwise identical conditions, an order-of-magnitude increase in current flow can be achieved in carefully designed magneto-electrolytic cells when the electric and magnetic fields are mutually perpendicular. Such enhancements have been interpreted, by means of magnetohydrodynamic models, and in terms of local vorticity generation in the neighbourhood of the electrodes. Equations for the prediction of mass transport enhancement have been developed for configurations where the analytical treatment of convective diffusion in boundary layers is not unduly complicated [1, 2].

It is well known in the classical theory of magnetohydrodynamics [3] that magnetic field superposition can suppress vorticity generation in certain configurations (the principle of an MHD

* Present address: Department of Business Administration, Harvard University, Cambridge, Mass., USA.

0021–891X/80/040481–08$02.80/0

nozzle, for instance, is based on this phenomenon). It may, therefore, be expected that under specific conditions the magnetic field can retard mass transport rates, generated in an electric field, by reducing ionic concentration gradients in the neighbourhood of the electrodes. On the basis of heat transport experiments conducted on horizontal mercury pools heated from below [4–7], such retardation effects on mass transport at horizontal cathodes facing upwards appear to be predictable by a logical application of similarity principles. For instance, using Chandrasekhar's theory of hydromagnetic stability [8], the retarding effect of the imposed magnetic field on the onset of hydrodynamic instability (i.e., the magnitude of the critical current density) in the cell can thus be estimated, provided that natural convection is the predominant mode of mass transfer. In the case of laminar forced-flow past a flat plate electrode, the distortion of velocity profiles may be estimated by applying the similarity principle to the analytical approach of Rossow [9] for heat transfer. In the above-quoted studies the common denominator is the collinear nature of the electric and magnetic fields; collinearity is responsible for the impeding effect on motion and, hence, transport rates (see Section 3).

In a practical magneto-electrolytic cell, natural and forced convection often co-exist and both contribute to the composite transport process; a numerical means of estimating such contributory effects has been proposed via the phenomenological concept of an interaction parameter [10, 12]. It is, of course, impossible to deduce from the numerical value of such a parameter the individual retardation effects exercised by the magnetic field on the natural-convective and forced-convective components. In order to gain insight into the individual retardation phenomena experimentally observed, decreases in mass transport rates have to be compared to decreases predicted via natural-convection and forced-convection models appropriately modified for the presence of collinear electric–magnetic fields.

The purpose of this paper is to present the results of such a study and to demonstrate how electrolytic mass transport rates can be reduced in magnetic fields. The phenomenon may find future application in selective co-deposition of metals on cathode surfaces and in related areas.

2. Experimental

The apparatus is sketched in Fig. 1. The electrolytic cell is a short section (6 cm long) of a long

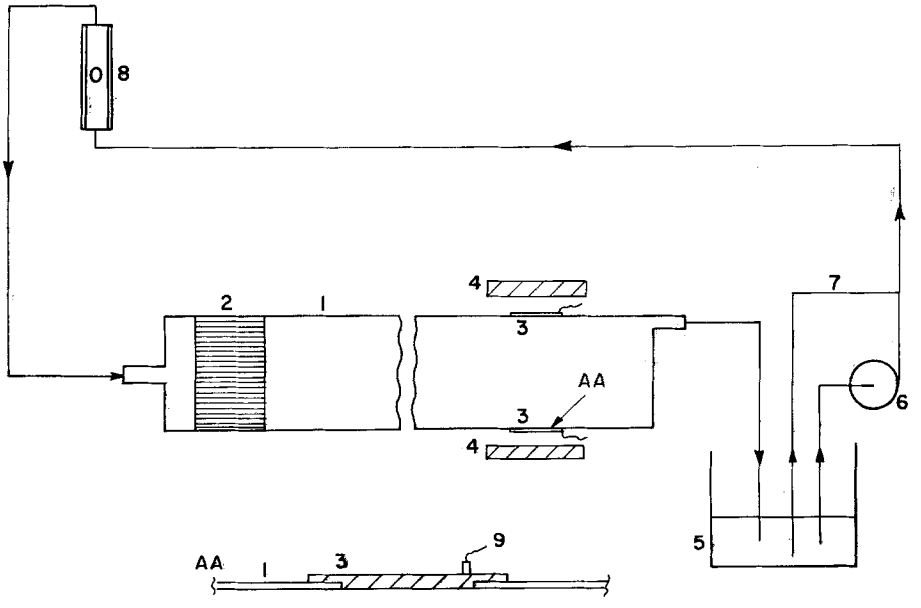

Fig. 1. Sketch of the experimental apparatus and electrode insertion (Section AA). 1 plastic cell wall; 2 parallel straws; 3 electrodes; 4 magnetic pole faces; 5 electrolyte holding tank; 6 circulating pump; 7 bypass line; 8 flowmeter; 9 electrode connection.

rectangular channel (total length: 247.5 cm), 2 cm wide and 4 cm deep; the associated hydrodynamic entry length required for the establishment of fully developed flow, is about 200 cm. The electrodes are 6.35 mm thick pure copper plates of dimensions 2 cm × 6 cm, set flush to the inner upper and lower channel surfaces, as shown in Section AA; they are easily removable for cleaning and pre-treatment. A tightly packed bundle of 6 cm long, 2.5 mm diameter plastic 'straws' was inserted at a 5 cm distance downstream from the channel entrance to accelerate flow-line stratification and the establishment of laminar flow conditions. The electrolyte, a mixture of aqueous solutions of 0.106 mol dm^{-3} $CuSO_4$ and 3.184 mol dm^{-3} H_2SO_4, was circulated between the channel, an 8 dm^3 reservoir and the rotameter-bypass assembly by means of a small plastic pump. The electrolytic cell section was placed between the pole faces of a 5 kV A Walker regulated d.c. electromagnet described in earlier communications [13]. D.c. electrolysis was carried out via a regulated HP standard bench-scale power supply (maximum rating of 4 A); the current–voltage variation was continuously monitored via an X–Y recorder and limiting currents were measured by a digital voltmeter/ammeter device. The electrode surfaces were carefully prepared before each run by sanding (120 grade and 240 grade sandpaper), degreasing with acetone and methanol, and drying. The potential difference across the cell was raised via a variable rheostat at the rate of 5 mV s^{-1} until the limiting current plateau was reached (usually at 0.7 V).

Table 1 contains a summary of experimental observations.

The limiting currents observed in the residual magnetic field are slightly higher in the second set (with the exception of the 385 cm^3 min^{-1} entry where the large deviation is unexplained), but within the usually expected experimental scatter. The electrolytic properties were estimated from standard handbook data, but the value of the diffusion coefficient was computed according to the procedure of Fenech and Tobias [14] which was judged to be more reliable at the employed H_2SO_4 concentration than the much earlier data of Cole and Gordon [15]. The flow rates were carefully selected to be within the laminar flow regime; very low flow rates were avoided for reasons of convenient flow control.

3. Theory

3.1. *Analysis in the absence of a magnetic field*

As mentioned before, the combined effect of natural and forced convection may conveniently be analyzed in terms of the interaction parameter, defined [10, 11] as

$$(Sh)/(Sh)_{NC} = \{1 + [(Sh)_{FC}/(Sh)_{NC}]^n\}^{1/n} \quad (1)$$

Equation 1 is written in terms of Sherwood num-

Table 1. Summary of the experimental results [23]. (Estimated electrolyte properties: $\nu = 0.015\,21$ cm^2 s^{-1}; $\sigma = 0.761$ $S\,cm^{-1}$; $D = 3.786 \times 10^{-6}$ cm^2 s^{-1} at $T = 20°$ C)

Volumetric flow rate, Q, (cm^3 min^{-1})	*Residence time, τ* (s)	*Limiting current flow, I_L* (mA)			
		$B = 4$ mT*	$B = 374$	$B = 685$	R_e†
355	8.108	81	–	73	129.73
370	7.782	84	–	75	135.17
525	5.484	87	–	78	191.80
660	4.364	92	–	78	241.10
720	4.000	93	–	81	262.98
800	3.599	93	–	83	292.30
385	7.481	103	97	85	140.61
430	6.696	103	91	72	157.09
600	4.800	101	92	88	219.15
720	4.000	102	93	89	262.98

* residual flux density.

† characteristic length: equivalent diameter of channel

bers, rather than current densities, pertaining to limiting (mass transport-control) conditions. The excess electrolyte effect on the Grashof number was considered via the procedure proposed by Newman and Selman [16], using their bisulphate model. The corresponding Sherwood numbers were computed via the relationships proposed by Goldstein [17] as 652.7; by Quraishi [18] as 486.71; by Lloyd and Moran [19] as 537.60; the characteristic length here is the length of the electrode. Since the first figure seems to be excessively high, the average of the remaining two, 512.15, was taken as the contribution of natural convection.

The contribution of forced convection was computed via the relationship of Pickett and Stanmore [20], expressed in terms of the characteristic electrode length

$$(Sh)_{FC} = 1.467 \left(\frac{2}{1+\gamma}\right)^{1/3} \left[(Re)_L (Sc) \frac{L}{d_e}\right]^{1/3}. \quad (2)$$

The experimental Sherwood numbers were computed as

$$(Sh) = \frac{i_L L}{zFDc_\infty} \quad (3)$$

since the transference number of copper ions is vanishingly small in the experimental system. Using Equation 1 and the 'template' plot shown in previous publications [10, 11], the interaction parameter is found to vary between 1/3 and unity, with a strong tendency to be between $n = 2/3$ and unity. It appears, therefore, that under experimental conditions natural convection is stronger than forced convection, the latter exhibiting, however, a significant contribution.

3.2. *The effect of the imposed magnetic field on mass transport*

The effect on the natural convection component will first be treated. Recalling that Chandrasekhar's theory [8] permits the estimation of retardation of the onset of flow instability in magnetic fields, the critical current density (see Appendix A) is computed to be 65.2 pA m^{-2} ($B = 374$ mT) and 80.2 pA m^{-2} ($B = 685$ mT); hence, at the experimental current flows the magnetic retardation effect is completely negligible. A similar finding follows from computing the effect of the magnetic field on the initial slope of the derivative of the universal function, $\bar{H}_1'(0)$, which determines the numerical value of the Sherwood number in the model of Rotem and Claassen [21]. As shown in Appendix A, the effect of the magnetic field is entirely negligible. One may conclude that the employed magnetic field strengths exert no sensible retardation effect on mass transport due to natural convection.

The effect on the forced-flow component is completely different. As shown in Appendix B, the magnetic field effect manifests itself by the quantity

$$\phi_m = k_1 - k_2 \frac{\sigma B_0^2}{\rho} \tau \quad (4)$$

indicating the quadratic effect of the magnetic field strength; the numerical values $k_1 = 1.33$ and $k_2 = 3.329$ pertain to the modified Rossow-model. Then, in the instance of flow between parallel plates,

$$(Sh)_L = 0.6783 \phi_m^{1/3} (Re)_L^{1/2} (Sc)^{1/3} \quad (5)$$

and for flow past flat plates,

$$(Sh)_L = 0.6183 \phi_m^{1/3} (Re)_L^{1/2} (Sc)^{1/3} \quad (6)$$

express the magnetic field effect on the dimensionless electrolytic mass transport rate. Equations 5 and 6 clearly indicate that as the magnetic flux density is increased, ϕ_m and hence $(Sh)_L$ become smaller; the numerical effect can be quite appreciable, as illustrated in Fig. 2 where experimentally observed relative mass transport rates are plotted against relative rates predicted by Equations 5 and 6. The slope of the least squares regression line, 1.009 88, is only slightly different from the diagonal slope of unity; since the computed likelihood ratio [22], 1.3, is much less than ten, it follows that the diagonal line is statistically indistinguishable from the least squares line and, as such, it can be accepted as a 'best' *linear* representation, with a standard error of estimate (root-mean square of the experimental deviations about the model) of 0.0692, although linear representation is not necessarily the most accurate. These results indicate that (a) the magnetic field retards forced flow, and (b) the retardation effect can be interpreted with reasonable confidence in

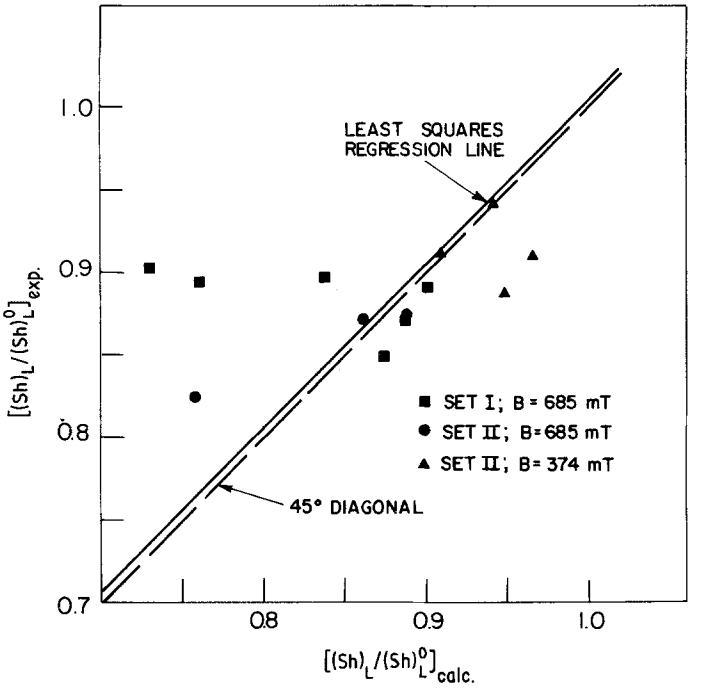

Fig. 2. Plot of the experimentally observed relative mass transport rates versus theoretically computed relative rates (for physical reasons the regression line passes through the 0,0 point).

terms of a flow-past-flat-plate model, appropriately modified for the presence of a magnetic field, which is transverse to the fully developed flow regime, but collinear with the electric field.

It is instructive to note that collinear electric and magnetic fields do not generate or suppress hydrodynamic flows in a continuum where the electric current flow and the magnetic flux are strictly uniform. This can be seen from Kelvin's theorem where the curl $(\mathbf{i} \times \mathbf{B}/\rho)$ becomes the null vector at such conditions. Thus, the magnetic field effect in the electrolyte bulk is most likely negligible and its influence is confined to the boundary layer existing at the electrode surfaces.

4. Concluding remarks

Magneto-electrolysis in collinear electric–magnetic fields, characterized by retardation of mass transport, is a counter-example to magneto-electrolysis with mass transport enhancement; the magnetic retardation effect is essentially confined to the forced-flow component. It may have practical usefulness in the simultaneous electrolysis of two or more ionic species, especially in separate liquid phases. This aspect will require further research and is beyond the scope of the current paper.

Appendix A

The magnetic field effect on the natural convective component

The estimation of the onset of flow instability via Chandrasekhar's theory. In his classical treatise [8], Chandrasekhar shows that the critical thermal Rayleigh number, associated with the onset of flow instability (i.e., convection), is a monotonically increasing function of the dimensionless parameter:

$$Q = \frac{\sigma d^2 B^2}{\rho \nu} \qquad \text{(A1)}$$

Thus, the retarding effect of the magnetic field on natural convection at horizontal flat plates facing upward is essentially quadratic, unless the magnetic field strength is very large. If Q is known, $(Ra)_{crit}$ may conveniently be obtained from graphs in Chandrasekhar's text.

Assuming 1 : 1 similarity between heat and mass transport, the critical current density may be estimated from $(Ra)_{crit}$ by replacing the thermal expansion coefficient with the conventional densification coefficient, and the thermal diffusion coefficient with the electrolyte diffusion coef-

ficient. In so doing, and under the conditions of the experimental work, $Q = 67.316B^2$; then, from Fig. 39, p. 171 in [8], one obtains $(Ra)_{crit} = 1905.5$ for $B = 374$ mT and $(Ra)_{crit} = 2344.2$ for $B = 685$ mT. The critical current densities are computed from the relationship

$$i_{crit} = \frac{zFD^2\nu}{g\alpha d^3}\left(\frac{10^3}{M}\right)(Ra)_{crit}. \qquad \text{(A2)}$$

Since, for the given electrolyte, $\alpha = 0.0123$, $M = 159.61$ and $z = 2$,

$$i_{crit} = 3.4205 \times 10^{-14}(Ra)_{crit} \qquad (\text{A m}^{-2})$$

whence $i_{crit} = 65.18\ \text{pA m}^{-2}$ ($B = 374$ mT) and $80.18\ \text{pA m}^{-2}$ ($B = 685$ mT).

The estimation of the magnetic field effect via the modified approach of Rotem and Claassen [21, 25]. In collinear electric and magnetic fields, the convective diffusion model [24] for a horizontal cathode facing upward, may be written as

$$v_x\frac{\partial v_x}{\partial x} + v_y\frac{\partial v_x}{\partial y} = -\frac{1}{\rho}\frac{\partial p}{\partial x} - \frac{\sigma v_x B_0^2}{\rho} + \nu\left(\frac{\partial^2 v_x}{\partial x^2} + \frac{\partial^2 v_x}{\partial y^2}\right) \qquad \text{(A3)}$$

$$v_x\frac{\partial v_y}{\partial x} + v_y\frac{\partial v_y}{\partial y} = -\frac{1}{\rho}\frac{\partial p}{\partial y} + \nu\left(\frac{\partial^2 v_y}{\partial x^2} + \frac{\partial^2 v_y}{\partial y^2}\right) + g\alpha\theta \qquad \text{(A4)}$$

$$v_x\frac{\partial \theta}{\partial x} + v_y\frac{\partial \theta}{\partial y} = D\left(\frac{\partial^2\theta}{\partial x^2} + \frac{\partial^2\theta}{\partial y^2}\right) \qquad \text{(A5)}$$

$$\frac{\partial v_x}{\partial x} + \frac{\partial v_y}{\partial y} = 0 \qquad \text{(A6)}$$

$$v_x = v_y = 0,\ \theta = 1 \text{ at } y = 0$$

$$v_x = v_y = \theta = 0 \text{ as } y \to \infty \qquad \text{(A7)}$$

The magnetic field effect is manifest by the second term on the right-hand side of Equation A3. Following the procedure of Rotem and Claassen the dimensionless mass transport rate may be computed as

$$(Sh) = \tfrac{5}{3}[-\bar{H}_1'(0)](Ra)^{1/5} \qquad \text{(A8)}$$

in the laminar flow regime. The numerical value of the derivative of the universal function $\bar{H}_1$ has been computed as -0.4601, in the absence of a magnetic field; the associated calculation involves a complicated trial-and-error solution of three differential equations written in terms of the universal functions obtained via undimensionalization and similarity transformation. In the presence of the magnetic field, this set may be written as

$$5\bar{F}_1''' - \bar{\gamma}\bar{F}_1' \cong 2[\bar{G}_1 - \bar{\eta}_1\bar{G}_1'] \qquad \text{(A9)}$$

$$\bar{H}_1 - \bar{G}_1' \cong 0 \qquad \text{(A10)}$$

$$\bar{H}_1'' + \tfrac{3}{5}\bar{F}_1\bar{H}_1' \cong 0 \qquad \text{(A11)}$$

$$\bar{F}_1 = \bar{F}_1' = 0;\ \bar{H}_1 = \bar{G}_1' = 1 \text{ at } \bar{\eta}_1 = 0$$

$$\bar{F}_1'' = \bar{H}_1 = \bar{G}_1 = 0 \text{ as } \bar{\eta}_1 \to \infty \qquad \text{(A12)}$$

The magnetic field effect is represented by the parameter

$$\bar{\gamma} = \frac{5}{9}\frac{\sigma\lambda^2 B_0^2}{\rho\nu(Ra)^{2/5}} \qquad \text{(A13)}$$

In the experimental system, $\bar{\gamma} = 0$ [10^{-3}] at most and, in consequence, the damping effect of the $\bar{\gamma}\bar{F}_1'$ term on Equation A9 is extremely small. The numerical solution of Equations A9–A12 shows that $\bar{H}_1'(0)$ is essentially -0.460, as in the $\bar{\gamma} = 0$ case.

Appendix B

The magnetic field effect on the forced-flow component

The analysis is a modification for collinear electric–magnetic fields of the approach by Rossow [9], shown also by Bopp [26], combined with the appropriate convective-diffusion model [27] of forced flow past a flat plate. The hydrodynamic regime is described by the equation system

$$v_x\frac{\partial v_x}{\partial x} + v_y\frac{\partial v_x}{\partial y} + \frac{\sigma B_0^2}{\rho}v_x = \nu\frac{\partial^2 v_x}{\partial y^2} \qquad \text{(A14)}$$

$$v_x = v_y = 0 \text{ at } y = 0 \qquad \text{(A15)}$$

$$v_x \to v_\infty;\ v_y \to 0;\ \frac{\partial v_x}{\partial y} = 0;\ \frac{\partial v_x}{\partial x} = -\frac{\sigma B_0^2}{\rho} \text{ as } y \to \infty \qquad \text{(A16)}$$

The solution of Equations A14–A16 yields the velocity field in the associated boundary layer.

Following Rossow's analysis, the velocity components may be written as

$$v_x \cong \frac{v_\infty}{2}\phi_m\eta \text{ and } v_y \cong \frac{1}{2}(v_\infty\nu/x)^{1/2}\frac{\phi_m}{2!}\eta^2 \quad \text{(A17)}$$

where the similarity variable is defined as $\eta = \frac{1}{2}(v_\infty/\nu x)^{1/2}y$.

Assuming that Equation A17 applies to the concentration boundary layer, the convective diffusion equation may be solved in the same manner as shown by Levich [27] in the absence of the magnetic field, as

$$(Sh) = 0.618\,34\,\phi_m^{1/3}(Re)_L^{1/2}(Sc)^{1/3} \quad \text{(A18)}$$

ϕ_m comprises the magnetic field effect; for small magnetic field strength, Rossow's results may be summarized as

$$\phi_m = 1.33 - 3.3291\frac{\sigma B_0^2}{\rho}\tau \quad \text{(A19)}$$

upon a proper regression analysis of his numerical data; the standard error of estimate for Equation A19 is 0.0026.

In the instance of laminar flow past parallel plates, the model by Pickett and Stanmore [20] has been modified by replacing their original velocity profile, β, with Rossow's; hence,

$$\beta = \frac{\phi_m}{4}\frac{v_\infty^{3/2}}{(\nu x)^{1/2}} \quad \text{(A20)}$$

is taken for further development. It then follows that if the classical Leveque approximation to the mass transfer coefficient is accepted, the local Sherwood number may be written as

$$(Sh)_x = 1.12 d_e\left(\frac{\beta}{9Dx}\right)^{1/3} \quad \text{(A21)}$$

where β is given by Equation A20. By substitution and appropriate rearrangement Equation A21 may be expressed as

$$(Sh)_x = 0.339\,14\,\phi_m^{1/3}(Re)^{1/2}(Sc)^{1/3}\,(d_e/x)^{1/2} \quad \text{(A22)}$$

The value of (Sh), averaged over the electrode length, is obtained upon integration as

$$(Sh) = 0.6783\,\phi_m^{1/3}(Re)^{1/2}(Sc)^{1/3}\,(d_e/L)^{1/2} \quad \text{(A23)}$$

Rewriting in terms of the characteristic electrode length,

$$(Sh)_L = 0.6783\,\phi_m^{1/3}(Re)_L^{1/2}(Sc)^{1/3} \quad \text{(A24)}$$

which is Equation 5. In the absence of the magnetic field and in view of the experimental conditions [$\gamma = 2.0$; $(Sc) = 4045.05$; $d_e = 2.67$ cm and $L = 6$ cm],

$$(Sh)_L = 11.885(Re)_L^{1/2} \quad \text{(A25)}$$

whereas the modified form of the Pickett–Stanmore equation (Equation 7, [20])

$$(Sh)_L = 1.467\left(\frac{2}{1+\gamma}\right)^{1/3}[(Re)_L(Sc)(L/d_e)]^{1/3} \quad \text{(A26)}$$

yields

$$(Sh)_L = 26.757\,(Re)_L^{1/3} \quad \text{(A27)}$$

The discrepancy between Equations A25 and A27 is not larger than about 20% on an average, in the experimental (Re) range. Note that the forcing of the Rossow-profile on the Leveque approximation leads to a square-root dependence of $(Sh)_L$ on $(Re)_L$ (in contrast with the cube-root dependence manifest in the Pickett–Stanmore analysis) because of the assumption that the separation distance between the two electrodes is large enough to ignore the effect of the anode on the hydrodynamic behaviour at the cathode.

References

[1] T. Z. Fahidy, *Chem. Eng. J.* 7 (1974) 21.
[2] Idem, *ibid* 17 (1979) 245.
[3] J. A. Shercliff, 'A Textbook of Magnetohydrodynamics', Pergamon Press (1965) Ch. 4.
[4] S. Chandrasekhar, *Phil. Mag.* 7 (43) (1952) 501.
[5] Y. Nakagawa, *Proc. Roy. Soc.* A240 (1957) 108.
[6] S. Chandrasekhar, *Phil Mag.* 7 (45) (1954) 1177.
[7] B. Lehnert and N. C. Little, *Tellus* 9 (1957) 97.
[8] S. Chandrasekhar, 'Hydrodynamic and Hydromagnetic Stability', Clarendon Press, Oxford (1961).
[9] V. J. Rossow, 'On Flow of Electrically Conducting Fluids Over a Flat Plate in the Presence of a Transverse Magnetic Field', *Natl. Adv. Comm. Acron.* Report no. 1358 (1958).
[10] S. Mohanta and T. Z. Fahidy, *Electrochim. Acta* 21 (1976) 143.
[11] *Idem, ibid* 21 (1976) 149.
[12] S. W. Churchill, *Amer. Inst. Chem. Eng. J.* 23 (1977) 10.
[13] S. Mohanta and T. Z. Fahidy, *Canad. J. Chem. Engrg.* 50 (1972) 248.
[14] E. J. Fenech and C. W. Tobias, *Electrochim. Acta* 2 (1960) 311.

[15] A. F. W. Cole and A. R. Gordon, *J. Phys. Chem.* **40** (1936) 733.
[16] J. R. Selman and J. Newman, *J. Electrochem. Soc.* **118** (1971) 1070.
[17] R. J. Goldstein, E. M. Sparrow and D. C. Jones, *Int. J. Heat Mass Transfer* **95** (1973) 405.
[18] M. S. Quraishi, PhD thesis, University of Waterloo (1978).
[19] J. R. Lloyd and W. R. Moran, *J. Heat Transfer* **96** (1974) 443.
[20] D. J. Pickett and B. R. Stanmore, *J. Appl. Electrochem.* **2** (1972) 151.
[21] Z. Rotem and L. J. Claassen, *Canad. J. Chem. Engrg.* **47** (1969) 461.
[22] P. M. Reilly, *ibid* **48** (1970) 168.
[23] T. S. Rutherford, Project Report, University of Waterloo (1979).
[24] V. G. Levich, 'Physicochemical Hydrodynamics' Prentice Hall (1962) Section 23.
[25] Z. Rotem and L. J. Claassen, *J. Fluid Mech.* **39** (1969) 173.
[26] G. R. Bopp, *Chem. Engrg. Prog.* **63** (10) (1967) 74.
[27] V. G. Levich, 'Physicochemical Hydrodynamics' Prentice Hall (1962) Section 15.